msec. However, complete (to within 1% of the final transmission) coloration and bleaching occur within 150 and 280 msec, respectively. From a perceived contrast point of view for a black-on-white display, coloration and bleaching times are about 50 and 200 msec, respectively. It should be noted that the response shown is not obtained immediately on operation of a freshly deposited SIROF, but only after the film has swelled by hydration (11). The temperature dependence of the response time of a SIROF, deposited under slightly different conditions from those described here, has been reported elsewhere (12).

Conclusions

Electrochromic iridium oxide films have been deposited by reactive sputtering from an Ir target in a pure O_2 plasma. Under the deposition conditions described here, films which could be completely bleached to zero absorbance (at -0.2V *vs.* SCE in 0.5M H_2SO_4) have been prepared. The colored state of these films is black, and a continuous charge or voltage selectable gray scale is available. These films could be switched through an optical density change of 0.3 in either direction in 40 msec under potentiostatic address; use of *IR* compensated potentiostatic address (10) can reduce this response time to 20 msec in either direction. Useful low temperature response times are also shown, *e.g.,* 0.25 sec at -10°C, when *IR* compensation is used to eliminate the effect of increased electrolyte resistivity. The energy requirement per color/bleach cycle for films as described here which show a single pass ΔOD of 0.48 (0.96, or a contrast ratio of 9:1, in a device configuration) is 38 mJ cm^{-2} cycle^{-1} at a response time down to 40 msec. Although this energy requirement is 20% greater than that for an AIROF (due to the 20% larger voltage window utilized with the same charge density for the same contrast), it is close to the requirement of a stable (nonaqueous) WO_3 half-cell for the same contrast but at a slower response time ($\sim$0.3 sec). Of course, in many applications a lower contrast is acceptable, permitting the use of a thinner film, with the energy requirement linearly dependent on the required ΔOD. SIROF's deposited under conditions close, but not identical, to those described here have undergone cycle lifetime testing both at room temperature and at elevated temperature in 0.5M H_2SO_4 electrolyte. At room temperature 2×10^7 full color/bleach cycles (with approximately 50% of that time with the SIROF having reached either the fully colored or fully bleached state) were obtained without perceived change in contrast, although a decrease in ΔQ and ΔOD of about 3% was recorded. Under the same conditions at 73°C, 2.5×10^5 cycles were obtained with a 5% decrease in ΔQ and ΔOD. Although similar life-testing of SIROF's deposited exactly as described in this work has not been performed, preliminary data show no significant difference.

Acknowledgment

We wish to acknowledge the expert assistance of Mrs. A. A. Pritchard, particularly in the SIROF deposition and electrode fabrication and the continued technical support of J. J. Wiegand.

Manuscript submitted Sept. 25, 1980; revised manuscript received Jan. 8, 1981.

Any discussion of this paper will appear in a Discussion Section to be published in the December 1981 JOURNAL. All discussions for the December 1981 Discussion Section should be submitted by Aug. 1, 1981.

Publication costs of this article were assisted by Bell Laboratories.

REFERENCES

1. S. Gottesfeld, J. D. E. McIntyre, G. Beni, and J. L. Shay, *Appl. Phys. Lett.,* **33,** 208 (1978).
2. G. Beni and J. L. Shay, *ibid.,* **33,** 567 (1978).
3. S. Gottesfeld and J. D. E. McIntyre, *This Journal,* **126,** 742 (1979).
4. G. Beni, C. E. Rice, and J. L. Shay, *ibid.,* **127,** 1342 (1980).
5. J. L. Shay, G. Beni, and L. M. Schiavone, *Appl. Phys. Lett.,* **33,** 942 (1978).
6. W. C. Dautremont-Smith, G. Beni, L. M. Schiavone, and J. L. Shay, *ibid.,* **35,** 565 (1979).
7. J. D. E. McIntyre, W. F. Peck, and S. Nakahara, *This Journal,* **127,** 1264 (1980).
8. L. M. Schiavone, W. C. Dautremont-Smith, G. Beni, and J. L. Shay, *Appl. Phys. Lett.,* **35,** 823 (1979).
9. G. Beni, L. M. Schiavone, J. L. Shay, W. C. Dautremont-Smith, and B. S. Schneider, *Nature,* **282,** 281 (1979).
10. W. C. Dautremont-Smith, L. M. Schiavone, G. Beni, and J. L. Shay, SID 1980 Digest, p. 122.
11. S. Hackwood, W. C. Dautremont-Smith, G. Beni, L. M. Schiavone, and J. L. Shay, *This Journal,* **128,** 1212 (1981).
12. S. Hackwood, G. Beni, W. C. Dautremont-Smith, L. M. Schiavone, and J. L. Shay, *Appl. Phys. Lett.,* **37,** 965 (1980).

Chemical Etching Characteristics of (001)InP

Sadao Adachi and Hitoshi Kawaguchi

Nippon Telegraph and Telephone Public Corporation,
Musashino Electrical Communication Laboratory, Musashino-shi, Tokyo 180, Japan

ABSTRACT

The chemical etching characteristics of (001)InP are studied through an SiO_2 mask in the solutions of various etching systems: (*i*) HCl, (*ii*) HCl:HNO_3, (*iii*) HBr, (*iv*) H_2SO_4:H_2O_2:H_2O, and (*v*) Br_2:CH_3OH. The etched depth is evaluated by using a calibrated optical microscope. The etching profiles are examined by cleaving the wafer in orthogonal directions along the (110) and $(\bar{1}10)$ planes. Various etching profiles, such as V-shaped, reverse mesa-shaped ones, and nearly vertical walls, are formed by stripes being etched on the (001) planes. The indexes of the etch-revealed planes are identified by making a comparison with the calculated angle between the (001) surface and etch-side plane. The utility of these etching solutions is also discussed for a variety of InP device applications.

Chemical etching of single crystal semiconductors plays an essential role in microelectronic solid-state device technology. Of the compound semiconductors, GaAs is most widely used in solid-state devices for specialized applications. Most of the data on etching of

Key words: chemical etching, InP, etching profile.

GaAs that one can find in the literature (1) involve studies of the mechanisms and kinetics of the dissolution processes. Tarui *et al.* (2) have reported in detail preferential etching characteristics of GaAs in the $Br_2:CH_3OH$ system and have then demonstrated geometrically etched profiles produced in the {001} and {111} planes by employing this system. They have also reported a few examples of practical applications of preferential etching (etching profile) for the device-structure design and fabrication.

InP and its related compounds, such as InGaAsP, are thought to be promising materials for high-speed transistors (IC's) and electrooptical devices. There have been a few reports on the etching characteristics of InP (3-7). Tuck and Baker (4) have studied etching characteristics of InP from crystallographic aspects, *e.g.*, orientation effects on etching rates, shapes of pits and hillocks, and dissolution processes. Huber and Linh (5) have studied defect delineation in InP by using specific etchants. However, to our knowledge, there has been no report on device shaping for InP using preferential etching.

In the present paper, we report chemical etching characteristics of the (001) surface of InP in the solutions of various systems: (i) HCl, (*ii*) $HCl:HNO_3$, (*iii*) HBr, (*iv*) $H_2SO_4:H_2O_2:H_2O$, and (*v*) $Br_2:CH_3OH$ systems. The etching profiles are examined by cleaving the (001) InP wafer in orthogonal directions along the (110) and $(\bar{1}10)$ planes and are discussed in detail from a crystallographic aspect. The profiles applicable to device-structure design and fabrication are also discussed.

Experimental

Sample.—The InP crystals employed were undoped single crystals grown by the liquid encapsulated Czochralski method. All wafers used were of (001) surface orientation with an uncertainty of 1° or less. These wafers were lapped and polished with fine abrasive alumina (0.05 μm particle size). After being degreased and rinsed in deionized water, they were chemically polished to a mirrorlike finish in a $Br_2:CH_3OH$ solution at room temperature. The thickness of these wafers was about 100 μm to permit cleavage for the observation of etching profiles.

Masking pattern.—Etching studies were performed for the etching-selected regions of (001) surface InP through windows in an SiO_2 mask (see Fig. 1). The SiO_2 masks used were approximately 2000Å thick and were prepared with conventional sputtering equipment. The desired geometries, in this case the window width of 30 μm wide, were defined by standard photolithography technique using AZ-1350 and an SiO_2 etchant of the $HF:NH_4F:H_2O$ system.

Etching solution.—The etching solutions employed can be classified into the following five groups: (*i*) HCl system (HCl, $HCl:CH_3COOH$, etc), (*ii*) $HCl:HNO_3$ system, (*iii*) HBr system (HBr, $HBr:CH_3COOH$, etc), (*iv*) $H_2SO_4:H_2O_2:H_2O$ system, and (*v*) $Br_2:CH_3OH$ system. The chemicals used were all of reagent grade. They were as follows: HCl (12*N*), H_2O_2 (30%), CH_3COOH (17*N*), H_3PO_4 (15*N*), HNO_3 (14.5*N*), HBr (9*N*), H_2SO_4 (36*N*), $K_2Cr_2O_7$ (purity $\geqq$ 99.8%), Br_2 (purity $\geqq$ 99%), CH_3OH (purity 99.5%), and H_2O (deionized water). A large quantity of solution was prepared to prevent the etching temperature from rising and the etch-solution composition from varying during the experiments. Etching was carried out in a temperature-controlled water vessel without illumination. The etchant was freshly mixed prior to each experiment. Etching experiments were done by stirring by hand.

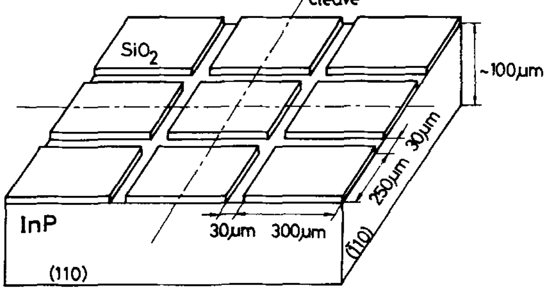

Fig. 1. An SiO_2 masking pattern on (001)InP wafer for chemical etching. The etching profiles are obtained by cleaving the wafer in orthogonal directions along the (110) and $(\bar{1}10)$ planes.

Etched depth and etching profile.—After etching, removing the SiO_2 mask, and rinsing in deionized water, the {110} plane perpendicular to the etched one was cleaved with a razor blade and the etched depths of samples were measured with a calibrated optical microscope. The etched depths were also measured from a step height between the etched and unetched surfaces using an interference microscope. Etching profiles were observed on the (110) and $(\bar{1}10)$ cleavage planes perpendicular to the wafer surface under an optical microscope.

Etching Profile

Etch figure.—Figure 2 includes a photograph of etch figures developed on the (001) plane of InP in the $H_2SO_4:H_2O_2:H_2O$ system, where the etch figures were

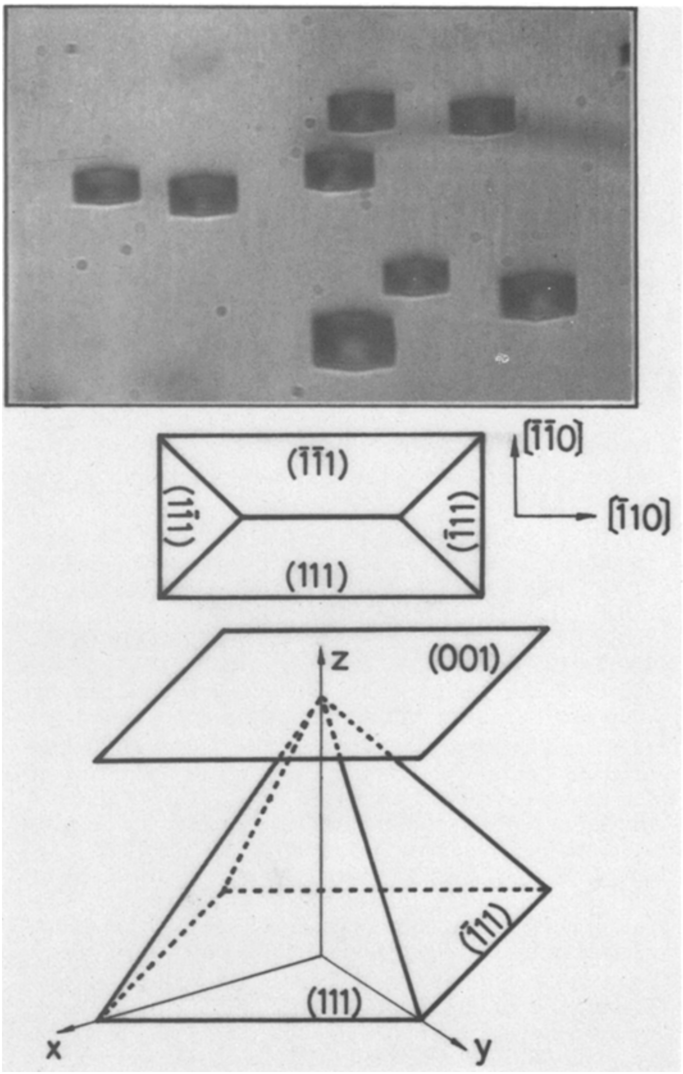

Fig. 2. Etching figures produced on the (001) plane of InP and schematic diagram of the individual etch figures.

produced by etching in the solution through pin-hole windows in an SiO_2 mask. A schematic diagram of the individual etch figures is also shown in the figure. The etch figures exhibit a rectangle-like (elongated) shape.

An important aspect of the arrangement of zincblende type crystals such as InP is the absence of a center of symmetry or inversion. Let the two sublattices of III-V compounds be labeled A^{III} and B^{V}. The A^{III}-B^{V} layers have unique orientations along the <111> crystal direction. The opposed (111) and $(\bar{1}\bar{1}\bar{1})$ faces and opposed [111] and $[\bar{1}\bar{1}\bar{1}]$ directions may have different physical and chemical properties. Such different properties are known to arise from crystallographic polarity. If a unit cell is chosen such that the B^{V} atoms are situated at its corner, then the B{111} planes may be referred to as $(\bar{1}\bar{1}\bar{1})$, $(11\bar{1})$, $(1\bar{1}1)$, and $(\bar{1}11)$, while the A{111} planes will be the corresponding negatives, *i.e.*, (111), $(\bar{1}\bar{1}1)$, $(\bar{1}1\bar{1})$, and $(1\bar{1}\bar{1})$. The pit figures can be successfully interpreted by a geometry constructed from the {111} planes, as shown in the middle and lower parts of Fig. 2. The elongated pits, similar to those of Fig. 2, have also been found in III-V compounds such as GaAs (2, 8), InSb (9), and InP (4). Gatos and Lavine (9) have revealed after geometric examination that the etch figures on (001)InSb are truncated (flat-bottomed) tetragonal pyramid structures, the four sides being {111} planes. The top plane of the truncated pyramid is either flat {100} or has higher order planes ({411}) forming a shallow angle with the <100> direction ($\simeq$ 19°). Olsen *et al.* (8) have also observed in SEM photographs the truncated tetragonal pyramid etch figures on (100)GaAs. Tuck and Baker (4), on the other hand, have observed untruncated tetragonal pyramid etch pits on (100)InP, where the $(11\bar{1})$ and $(1\bar{1}\bar{1})$ planes meet in a ridge at the bottom of the pit. From careful inspection using a differential interference microscope, we have also found that the pit figures on (001)InP have untruncated tetragonal pyramid structures, as shown schematically in the middle part of Fig. 2. The elongated etch figures demonstrate the nonequivalence of <110> and $<\bar{1}10>$ type directions lying in a {001} plane in the III-V intermetallic compounds. As mentioned before, this nonequivalence is known to arise from the <111> crystallographic polarity of zincblende type crystal. Elongated etch figures, thus, provide us a means for the unique determination of crystallographic directions between the <110> and <110> type directions.

HCl system.—The etching profiles of (001)InP etched in the solutions of the HCl system are shown in Fig. 3: (a) HCl (25°C, 1 min), (b) $1HCl:1H_2O_2$ (25°C, 1 min), (c) $1HCl:1CH_3COOH$ (25°C, 1 min), (d) $1HCl:1H_3PO_4$ (25°C, 1 min), (e) $1HCl:1CH_3COOH:1H_2O_2$ (25°C, 1 min), and (f) $1HCl:1H_3PO_4:1H_2O_2$ (25°C, 1 min). The cross sections are obtained by cleaving the wafers in orthogonal directions along the (110) and $(\bar{1}10)$ planes (see Fig. 1). The determination of crystallographic directions was made by means of the above-mentioned etch-figure test. It is clear from the figure that the etching profiles change in shape with a crystallographic rotation of 90° about the [001] axis and that they exhibit crystal habits. In the case of the (110) cleavage planes, the etching profiles indicate planes are nearly perpendicular to the (001) surface and inclined planes slope downward away from the SiO_2 mask. In the case of the $(\bar{1}10)$ cleavage planes, the profiles indicate only the inclined planes whose sides form angles of about 35° [(a), (c), and (d)] or 55° [(b), (e), and (f)] with respect to the (001) surface. Consequently, the etching profile of the $(\bar{1}10)$ cleavage plane [Fig. 3(a)] clearly shows a V-shaped groove profile forming a V-groove angle of 110° (angle between two inclines). If the etching time is properly chosen according to the V-groove width, depth, and corresponding etching rate, one can also easily fabricate the V-shaped groove in the $<\bar{1}10>$ direction on (001)InP by chemical etching in solutions such as $1HCl:1H_2O_2$ and $1HCl:1CH_3COOH:1H_2O_2$ (V-groove angle of 70°).

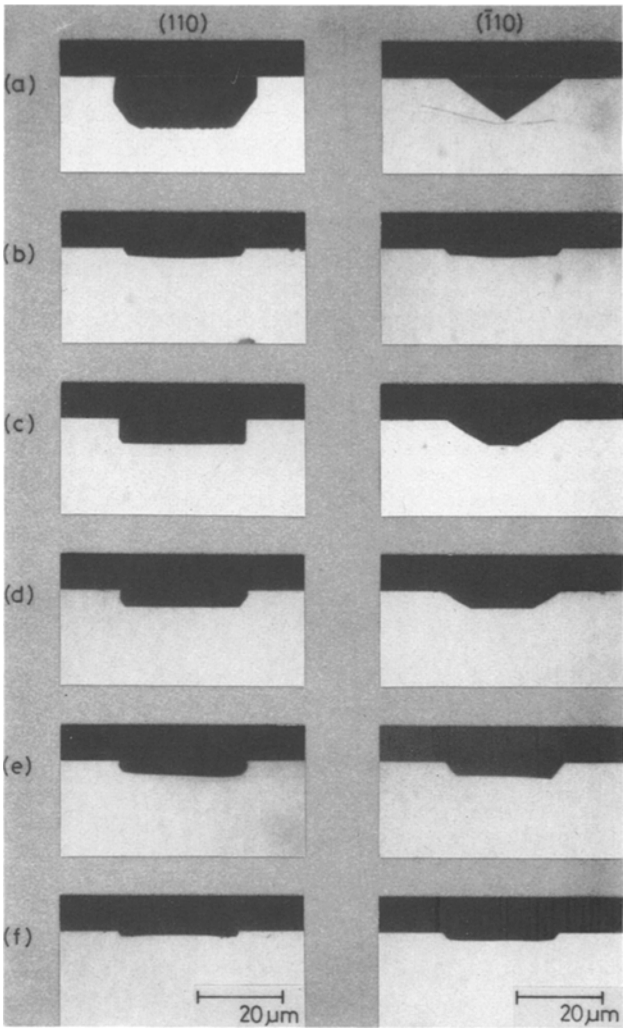

Fig. 3. Etching profiles of (001)InP etched in the solutions of the HCl system: (a) HCl (25°C, 1 min), (b) $1HCl:1H_2O_2$ (25°C, 1 min), (c) $1HCl:1CH_3COOH$ (25°C, 1 min), (d) $1HCl:1H_3PO_4$ (25°C, 1 min), (e) $1HCl:1CH_3COOH:1H_2O_2$ (25°C, 1 min), and (f) $1HCl:1H_3PO_4:1H_2O_2$ (25°C, 1 min).

HCl:HNO₃ system.—The etching profiles of (001)InP etched in the solutions of the $HCl:HNO_3$ system are shown in Fig. 4: (a) $1HCl:1HNO_3$ (25°C, 1 min), (b) $1HCl:2HNO_3$ (25°C, 1 min), (c) $2HCl:1HNO_3$ (25°C, 1 min), (d) $1(1HCl:1HNO_3):1H_2O$ (25°C, 1 min), (e) $1(1HCl:1HNO_3):1H_2O_2$ (25°C, 1 min), and (f) $1(1HCl:1HNO_3):1CH_3COOH$ (25°C, 1 min). The etching profiles of the (110) cleavage planes [Fig. 4(a), (b), (c), and (f)] indicate the planes are nearly perpendicular to the (001) surface, similar to those of the HCl system. The profile of the $(\bar{1}10)$ cleavage plane [Fig. 4(c)] indicates the inclined planes forming an angle of 35° with respect to the (001) surface, but those of Fig. 4(a) and (b) do not exhibit clear crystal habits. If one chooses proper etching time, the $2HCl:1HNO_3$ solution also makes it possible to fabricate a V-shaped groove whose sides form an angle of 110° (*i.e.*, an angle of V-shaped groove). As one can see in Fig. 4(d), (e), and (f), the etching rate reduced abruptly with an addition of H_2O, H_2O_2, or CH_3COOH in the solution of the HCl:HNO_3 system [see also Table I].

HBr system.—The etching profiles of (001)InP etched in the solutions of the HBr system are shown in Fig. 5: (a) HBr (25°C, 1 min), (b) 1HBr:$1H_2O_2$ (25°C, 1 min), (c) 1HBr:$1CH_3COOH$ (25°C, 1 min), (d) 1HBr:$1H_3PO_4$ (25°C, 1 min), (e) 1HBr:$1HNO_3$ (25°C, 1 min), and (f) 1HBr:$1HNO_3$:$5H_2O$ (25°C, 1 min). The profiles of Fig. 5(a) indicate the inclined planes for both the (110) and $(\bar{1}10)$ cleavage planes forming an angle of 55° with respect to the (001) surface. The side-etch speed of the (110) cleavage plane is faster than that of the $(\bar{1}10)$ cleavage plane. The cross sections demonstrated in Fig. 5(b) exhibit a reverse mesa-shaped and mesa-shaped profiles for the (110) and $(\bar{1}10)$ cleavage planes, respectively. The etched sides for the (110) and $(\bar{1}10)$ cleavage planes form angles of 125° and 55°, respectively, with respect to the (001) surface. Such profiles are quite similar to those on (001)GaAs etched with H_2SO_4:H_2O_2:H_2O (10) and Br_2:CH_3OH solutions (2). The profile shown in Fig. 5(c) [(110) cleavage plane] exhibits the reverse mesa-shaped and mesa-shaped structures in addition to the flat-bottomed plane. The reverse mesa-shaped and mesa-shaped planes form angles of 110° and 55°, respectively, with respect to the (001) surface. The profile of the $(\bar{1}10)$ cleavage plane [Fig. 5(c)], on the other hand, exhibits only the inclined planes forming an angle of 55° with respect to the (001) surface. Similar etching profiles have also been obtained by Otsubo *et al.* (11) on (001)GaAs with etching in a solution of the $C_3H_4(OH)(COOH)_3 \cdot H_2O$:$H_2O_2$:$H_2O$ system. The etching profiles of Fig. 5(d) are the same as those of Fig. 5(a). The profiles of Fig. 5(e) and (f) are also quite similar to those of Fig. 5(b), but they do not reveal clear crystallographic planes.

H_2SO_4:H_2O_2:H_2O system.—The etching profiles of (001)InP etched in the solutions of the H_2SO_4 system are shown in Fig. 6: (a) $1H_2SO_4$:$1H_2O_2$ (60°C, 20 min), (b) $3H_2SO_4$:$1H_2O_2$:$1H_2O$ (60°C, 20 min), (c) $1H_2SO_4$:$1H_2O_2$:$1H_2O$ (60°C, 20 min), and (d) $3(2N\text{-}K_2Cr_2O_7)$:$1H_2SO_4$:1HCl (60°C, 20 min). The profiles of the (110) cleavage planes [Fig. 6(a)-(c)] indicate the planes are nearly perpendicular to the (001) surface, while those of the $(\bar{1}10)$ cleavage planes indicate the inclined sides that slope downward away from the SiO_2 mask. The profiles of the $(\bar{1}10)$ cleavage planes [Fig. 6(a) and (b)] exhibit the mesa-shaped structure, but they do not indicate clear crystal habits, in contrast to that of Fig. 6(c).

The H_2SO_4:H_2O_2:H_2O system is known to be one of the most commonly employed etchants for GaAs (11). Chemical polishing by using this system also gives high-quality GaAs surfaces of low-index orientations except for the Ga{111} surface. However, the etching rates of this system for InP are two or three orders smaller than those for GaAs. The system, moreover, sometimes produces elliptical etch pits on the (001) surface of InP. The photograph of the elliptical etch pits are demonstrated in the lower part of Fig. 6(c). The long- and short-axis directions of the ellipsoid correspond to the $[\bar{1}10]$ and [110] directions, respectively. The profile of the (110) cleavage plane of (001)InP etched in the solution of $3(2N\text{-}K_2Cr_2O_7)$:$1H_2SO_4$:1HCl [Fig. 6(d)] exhibits the mesa-shaped structure, in contrast to those of the H_2SO_4:H_2O_2:H_2O systems. The profile of the $(\bar{1}10)$ cleavage plane also exhibits the mesa-shaped structure (revealing clear crystal habits), as similar to those found in Fig. 6 (a)-(c). This etchant system produces etch-pit free surfaces and moreover provides high-quality InP surfaces. It was found that the etching rates of this system were increased by increasing HCl at a constant ratio of

Table I. The composition of the etchants in parts by volume, etching condition, etched depth, and identified crystallographic planes revealed by etching

Etchant	Etching condition: Time (min)	Etching condition: Temperature (°C)	Etched depth (μm)	Identified planes: (110)	Identified planes: $(\bar{1}10)$
HCl	1	25	12.0	$\{\bar{1}10\},\{\bar{1}11\}$	$\{\bar{1}\bar{1}2\}$
1HCl:$1H_2O$	1	25	0.07		
1HCl:$1H_2O_2$	1	25	2.3	$\{\bar{1}10\},\{\bar{1}11\}$	$\{\bar{1}\bar{1}1\}$
1HCl:$1CH_3COOH$	1	25	6.0	$\{\bar{1}10\}$	$\{\bar{1}\bar{1}2\}$
1HCl:$1H_3PO_4$	1	25	4.0	$\{\bar{1}10\},\{\bar{1}11\}$	$\{\bar{1}\bar{1}2\}$
1HCl:$1H_2O_2$:$1H_2O$	1	25	0.1		
1HCl:$1CH_3COOH$:$1H_2O_2$	1	25	4.0	$\{\bar{1}10\},\{\bar{1}11\}$	$\{\bar{1}\bar{1}1\}$
1HCl:$1H_3PO_4$:$1H_2O_2$	1	25	2.0	†	$\{\bar{1}\bar{1}1\}$
1HCl:$1HNO_3$	1	25	6.5	$\{\bar{1}10\}$	†
1HCl:$2HNO_3$	1	25	7.0	$\{\bar{1}10\}$	†
2HCl:$1HNO_3$	1	25	8.5	$\{\bar{1}10\},\{\bar{1}11\}$	$\{\bar{1}\bar{1}2\}$
1(1HCl:$1HNO_3$):$1H_2O$	1	25	0.15		
1(1HCl:$1HNO_3$):$1H_2O_2$	1	25	0.5	†	$\{\bar{1}\bar{1}1\}$
1(HCl:$1HNO_3$):$1CH_3COOH$	1	25	1.0	$\{\bar{1}10\}$	$\{\bar{1}\bar{1}2\}$
HBr	1	25	6.5	$\{\bar{1}11\}$	$\{\bar{1}\bar{1}1\}$
1HBr:$1H_2O_2$	1	25	23	$\{\bar{1}11\}$	$\{\bar{1}\bar{1}1\}$
1HBr:$1CH_3COOH$	1	25	3.0	$\{\bar{1}11\},\{\bar{2}21\}$	$\{0\bar{1}1\}$
1HBr:$1H_3PO_4$	1	25	2.0	$\{\bar{1}11\}$	$\{\bar{1}\bar{1}1\}$
1HBr:$1HNO_3$	1	25	11.0	†	$\{\bar{1}\bar{1}1\}$
1HBr:$1HNO_3$:$5H_2O$	1	25	9.0	†	†
$1H_2SO_4$:$1H_2O_2$	20	60	4.0	$\{\bar{1}10\}$	†
$3H_2SO_4$:$1H_2O_2$:$1H_2O$	20	60	3.5	$\{\bar{1}10\}$	†
$1H_2SO_4$:$1H_2O_2$:$1H_2O$	20	60	2.5	$\{\bar{1}10\}$	$\{\bar{1}\bar{1}1\}$
$3(2N\text{-}K_2Cr_2O_7)$:$1H_2SO_4$:1HCl	20	60	2.0	†	$\{\bar{1}\bar{1}1\}$
4% Br_2:CH_3OH	1	25	25	$\{\bar{1}11\}$	$\{\bar{1}\bar{1}1\}$
2% Br_2:CH_3OH	1	25	18	$\{\bar{1}11\}$	$\{\bar{1}\bar{1}1\}$
1% Br_2:CH_3OH	1	25	12	$\{\bar{1}11\}$	$\{\bar{1}\bar{1}1\}$
0.2% Br_2:CH_3OH	2	25	7.0	$\{\bar{1}11\}$	$\{\bar{1}\bar{1}1\}$
0.1% Br_2:CH_3OH	4	25	8.0	$\{\bar{1}11\}$	$\{\bar{1}\bar{1}1\}$

† Etching profile does not exhibit clear crystal habits.

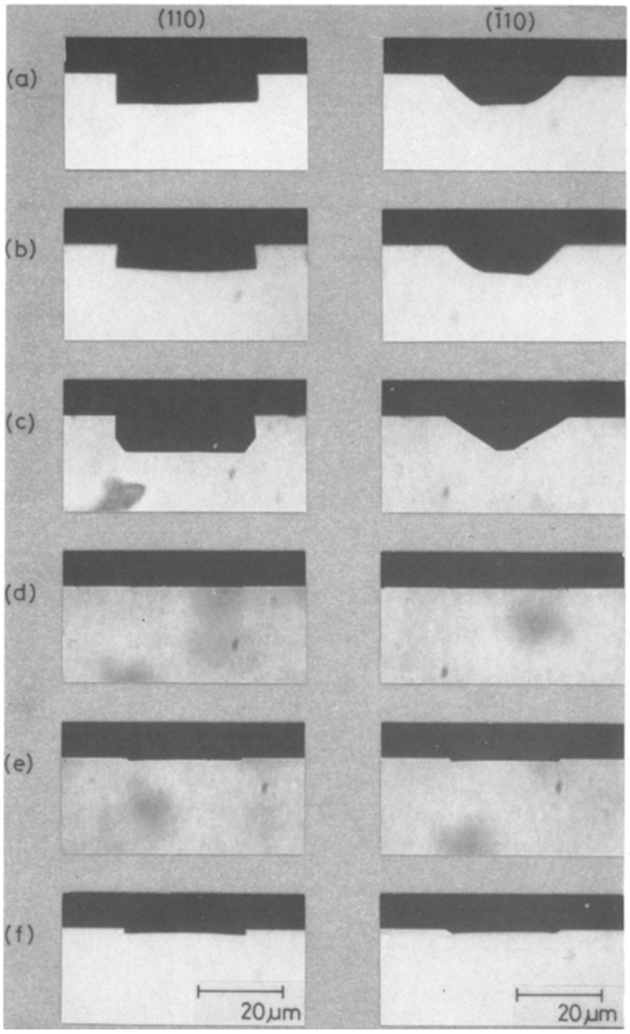

Fig. 4. Etching profiles of (001)InP etched in the solutions of the $HCl:HNO_3$ system: (a) $1HCl:1HNO_3$ (25°C, 1 min), (b) $1HCl:2HNO_3$ (25°C, 1 min), (c) $2HCl:1HNO_3$ (25°C, 1 min), (d) $1(1HCl:1HNO_3):1H_2O$ (25°C, 1 min), (e) $1(1HCl:1HNO_3):1H_2O_2$ (25°C, 1 min), and (f) $1(1HCl:1HNO_3):1CH_3COOH$ (25°C, 1 min).

$2N\text{-}K_2Cr_2O_7$ and H_2SO_4 without any change of the surfaces states; $\simeq 0.1$ μm/min [$3(2N\text{-}K_2Cr_2O_7):1H_2SO_4:1HCl$], $\simeq 1.0$ μm/min [$3(2N\text{-}K_2Cr_2O_7):1H_2SO_4:2HCl$], and $\simeq 2.0$ μm/min [$3(2N\text{-}K_2Cr_2O_7):1H_2SO_4:3HCl$] at 60°C. Details of these etching solutions will be presented in the near future.

$Br_2:CH_3OH$ system.—It is well known that the $Br_2:CH_3OH$ systems give good results for preferential etching of GaAs(2). The etching rates can be easily controlled by varying the Br_2 concentrations in CH_3OH. These systems are also usually employed as the etchants, capable of producing highly polished surfaces on GaAs. Figure 7 shows the etching profiles of (001)InP etched in the solutions of the $Br_2:CH_3OH$ system: (a) 4% by volume $Br_2:CH_3OH$ (25°C, 1 min), (b) 2% by volume $Br_2:CH_3OH$ (25°C, 1 min), (c) 1% by volume $Br_2:CH_3OH$ (25°C, 1 min), (d) 0.2% by volume $Br_2:CH_3OH$ (25°C, 2 min), and (e) 0.1% by volume $Br_2:CH_3OH$ (25°C, 4 min). The profiles of the (110) cleavage planes exhibit the reverse mesa-shaped structure forming an angle of 125° with respect to the (001) surface, while those of the $(\bar{1}10)$ cleavage planes exhibit the mesa-shaped structure forming an angle of 55° with respect to the (001) surface. Such features are quite similar to those of (001)GaAs etched with the $Br_2:CH_3OH$ (2) and $H_2SO_4:H_2O_2:H_2O$ systems (10). The profiles are also the same as those of InP etched with the $1HBr:1H_2O_2$ solution [see Fig. 5(b)].

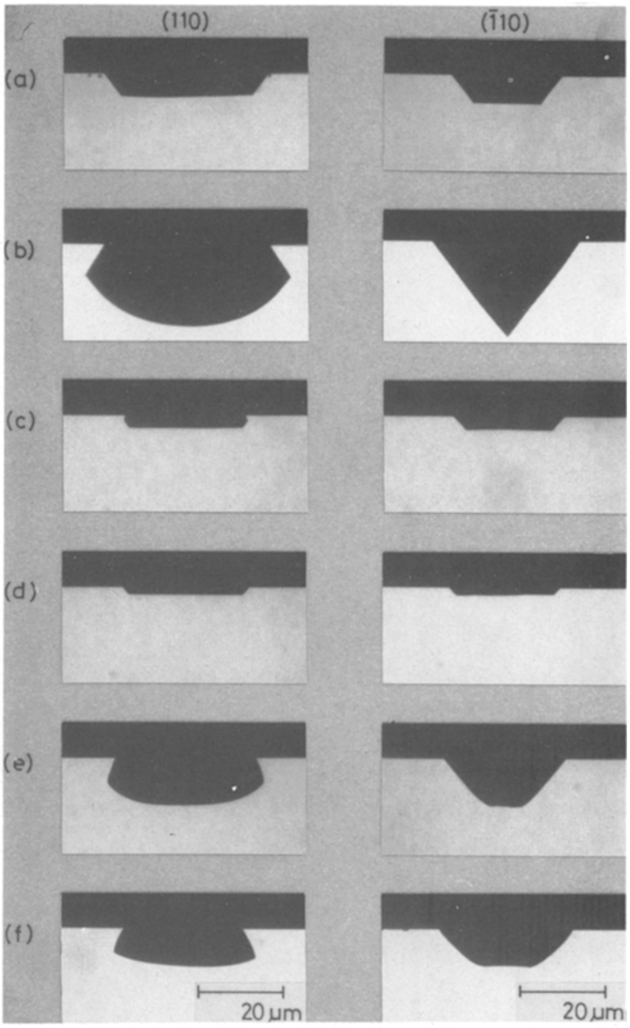

Fig. 5. Etching profiles of (001)InP etched in the solutions of the HBr system: (a) HBr (25°C, 1 min), (b) $1HBr:1H_2O_2$ (25°C, 1 min), (c) $1HBr:1CH_3COOH$ (25°C, 1 min), (d) $1HBr:1H_3PO_4$ (25°C, 1 min), (e) $1HBr:1HNO_3$ (25°C, 1 min), and (f) $1HBr:1HNO_3:5H_2O$ (25°C, 1 min).

The etching rates are found to vary from 2 μm/min (0.1% by volume) to 25 μm/min (4% by volume) with the Br_2 concentrations in CH_2OH.

Crystallographic aspect.—In this subsection, we discuss the etching profiles of (001)InP demonstrated in Fig. 3-7 from a crystallographic aspect. Figure 8 shows two-dimensional schematic representations of two orthogonal (110) and $(\bar{1}10)$ planes of a (001)InP layer. The open and solid circles indicate the In and P atoms, respectively. The (110) and $(\bar{1}10)$ planes, thus, represent the interchange of In-P atomic species of the zinc-blende type crystal InP upon a rotation of 90° about the [001] axis. The {001} surfaces, in principle, consist either of the In or P atoms. However, neither is preferred since both types are doubly bonded to the crystal lattice at the surface, and real {001} surfaces consist of a mixture of the In and P atoms. On the other hand, the intermetallic compound InP has two types of {111} surfaces, *i.e.*, In{111} and P{111} surfaces, resulting from the crystallographic polarity of the {111} directions. The outermost atom layer in each surface consists of either In or P atoms which are triply bonded to the crystal lattice. The In and P atoms have three and five bonding electrons per atom, respectively. The {111} surface In atoms have no spare electrons because they are all used up in hanging on to the crystal lattice. The {111} surface P atoms, on the other hand, have two electrons per atom available

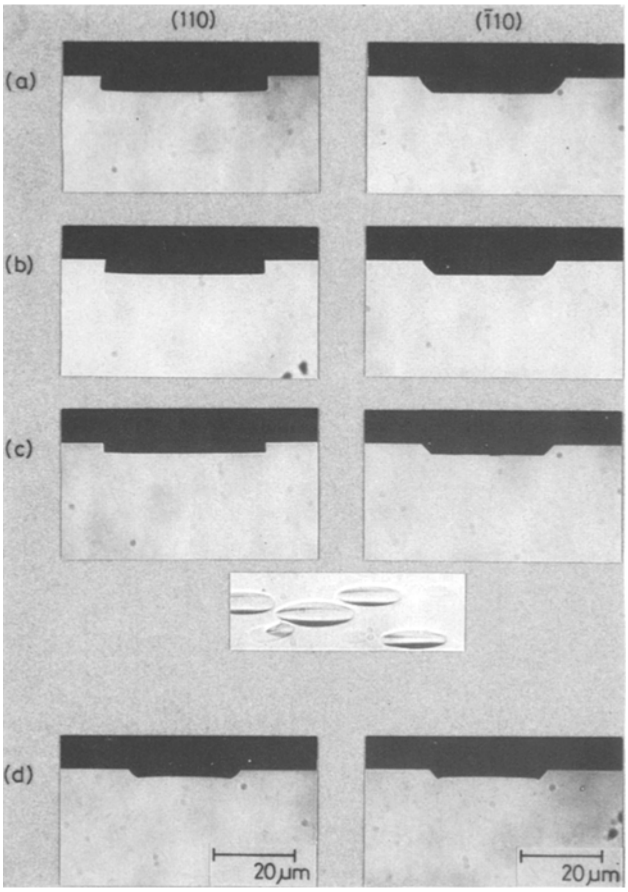

Fig. 6. Etching profiles of (001)InP etched in the solutions of the H_2SO_4 system: (a) $1H_2SO_4:1H_2O_2$ (60°C, 20 min), (b) $3H_2SO_4:1H_2O_2:1H_2O$ (60°C, 20 min), (c) $1H_2SO_4:1H_2O_2:1H_2O$ (60°C, 20 min), and (d) $3(2N\text{-}K_2Cr_2O_7):1H_2SO_4:1HCl$ (60°C, 20 min).

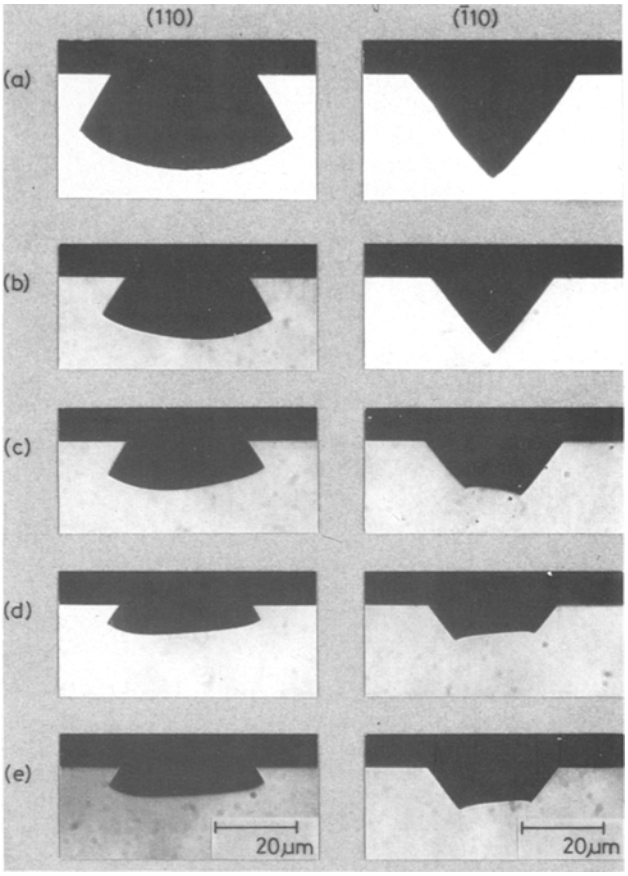

Fig. 7. Etching profiles of (001)InP etched in the solutions of the $Br_2:CH_3OH$ system: (a) 4% by volume $Br_2:CH_3OH$ (25°C, 1 min), (b) 2% by volume $Br_2:CH_3OH$ (25°C, 1 min), (c) 1% by volume $Br_2:CH_3OH$ (25°C, 1 min), (d) 0.2% by volume $Br_2:CH_3OH$ (25°C, 2 min), and 0.1% by volume $Br_2:CH_3OH$ (25°C, 4 min).

to take part in a reaction. Thus, the P{111} planes are very reactive compared with the In{111} planes.

From a viewpoint of crystallography, we can classify the etching profiles shown in Fig. 3-7 into the four individual groups, as demonstrated in Fig. 9. Details of two-dimensional schematic diagrams corresponding to Fig. 9(d) are also shown in Fig. 8. The etch-revealed walls perpendicular to the (001) surface, observed on the (110) cleavage plane in the solutions of the HCl, $HCl:HNO_3$, and $H_2SO_4:H_2O_2:H_2O$ systems, correspond to the $\{\bar{1}10\}$ crystallographic planes. The inclined planes forming an angle of 55° with respect to the (001) surface [see, *e.g.*, Fig. 5(a)] correspond to the In$\{\bar{1}11\}$ [(110) cleavage plane] and In{111} crystallographic planes [($\bar{1}$10) cleavage plane], where the $\{\bar{1}11\}$ or $\{\bar{1}\bar{1}1\}$ planes, in principle, form an angle of 54°44′ with respect to the {001} planes. The inclined plane forming an angle of 35° with respect to the (001), shown in Fig. 9(a), correspond to the In$\{\bar{1}\bar{1}2\}$ crystallographic planes [see, *e.g.*, Fig. 3(a)]. The $\{\bar{1}\bar{1}2\}$ planes, in principle, form an angle of 35°16′ with respect to the {001} planes. The etching profile of the (110) cleavage plane, shown in Fig. 5(c), is composed of two individual planes, forming angles of 109° and 55° with respect to the (001) surface, while that of the ($\bar{1}\bar{1}$0) cleavage plane exhibits only the mesa-shaped structure forming an angle of 45° with respect to the (001) surface. As shown in Fig. 9(c), the most probable planes deduced from these angles are In$\{2\bar{2}\bar{1}\}$ and In$\{\bar{1}11\}$ planes for the (110) cleavage plane and $\{0\bar{1}1\}$ planes for the ($\bar{1}$10) cleavage plane. The reverse mesa-shaped and V-shaped groove structures were formed on the (110) and ($\bar{1}$10) cleavage planes, respectively, with etchants such as $1HBr:1H_2O_2$ [Fig. 5(b)] and $Br_2:CH_3OH$ solutions (Fig. 7). These structures form angles of 125° (reverse mesa-shaped) and 55° (mesa-shaped) with respect to the (001) surface [Fig. 9(d)], which agree reasonably with angles between the {001} and $\{\bar{1}\bar{1}1\}$ planes. The etch-side planes can, thus, be identified to be the In$\{\bar{1}\bar{1}1\}$ planes (see Fig. 8). The etching proceeds up to the In{111} planes, because the P{111} planes are very reactive compared with the In{111} planes. Consequently, the reverse mesa-shaped and V-shaped groove structures are formed on the (110) and ($\bar{1}$10) cleavage planes, respectively, whose sides in principle form angles of 125°16′ and 54°44′ with respect to the (001) surface.

The dissolution process under consideration is far too complex and the available information rather limited to allow a quantitative development of the dissolution mechanism. Moreover, it is difficult to obtain a complete explanation of the difference in the etching profiles with various etching solutions. However, we suggest that this difference is due to the differences of the etching rates in the various crystallographic planes (*i.e.*, the slowest-etching-rate planes will play an important role on the etching profiles. The etch-side planes identified are summarized in Table I along with the etching time, temperature, and etched depth.

Proposed Device Application

The etching profiles obtained here should be very useful for the design and fabrication of electron and electrooptical devices. Comerford and Zory (12) have used selective etching techniques to fabricate V-groove

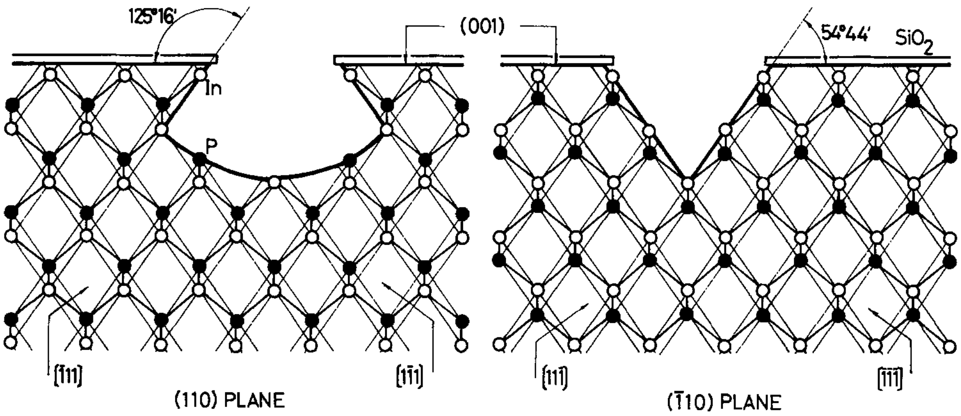

Fig. 8. Two-dimensional schematic representations of two orthogonal (110) and (1̄10) planes of a (001)InP layer. The open and solid circles indicate the In and P atoms, respectively. The round hole bottom on the left side is not necessarily the precise atomic configuration.

diffraction grating on the (001) surfaces of GaAs using the Br_2:CH_3OH solution as the preferential etchant. Tsang and Wang (13) have also fabricated the diffraction grating on the (001) surface of GaAs, where the H_2SO_4:H_2O_2:H_2O system has been used as the preferential etchant. The results demonstrated in this paper also indicate that the V-groove diffraction grating on the (001) surface of InP should be fabricated by chemical etching with proper choice of direction of grating-mask groove openings and controlling the width of the groove openings and/or etching time.

Gannon and Nuese (14) have discussed the utility of the NH_4OH:H_2O_2 preferential etchant for GaAs device preparation and have demonstrated its application to the fabrication of integrated GaAs bipolar transistors. The NH_4OH:H_2O_2 etchant has been found to provide a flat etching bottom and a slow etching rate for {001}GaAs, which led to the success of the transistor fabrication procedure. The etchants, such as the 1HCl:1CH_3COOH [Fig. 3(c)], 1HCl:1H_3PO_4 [Fig. 3(d)], 1HBr:1CH_3COOH [Fig. 5(c)], and 1HBr:1H_3PO_4 solutions [Fig. 5(d)], also provide a flat etching bottom and a relatively slow etching rate for {001}InP. These etchants should, therefore, be useful for producing high-quality InP transistors and IC's. The lateral definition, which is especially required and important in a number of passive optical components such as waveguides and directional couplers, can also be achieved by a chemical etching technique employing these solutions as the etchant.

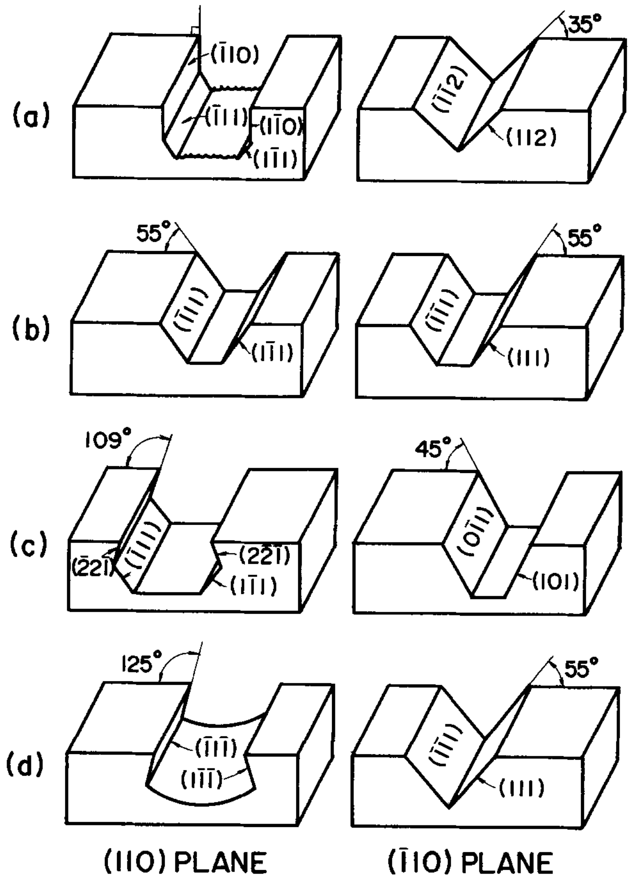

Fig. 9. Schematic diagrams of the etching profiles produced in the (001) planes of InP by the various etching solutions (see text).

Realization of monolithic integration of optical circuits will require a conventional means of routing optical signals on integrated chips (15). The fabrication of double heterostructure lasers, which incorporate chemically etched mirrors, has been reported to realize the monolithic fabrication of integrated optical devices (16, 17). In such works, much attention has been paid to produce smooth-mirror Fabry-Perot resonator by chemical etching because it improves the characteristics of laser diodes such as threshold current density, quantum efficiencies, and lasing modes. Therefore, in the fabrication of etched-mirror laser diodes, it is important to produce the vertical walls which give a high value of the mirror reflectivity. The etching solutions, such as the HCl (Fig. 3) and H_2SO_4:H_2O_2:H_2O systems (Fig. 6), are thought to be useful for the monolithic fabrication of etched-mirror laser diodes. Recently, Miller and Iga (17) have successfully fabricated InGaAs/InP laser diodes emitting at 1.3 μm by wet chemical etching with a solution of 1HCl:2CH_3COOH:1H_2O_2 [see Fig. 3(e)]. The geometric profiles are also applicable to the fabrication of lateral-confinement laser diodes such as the buried-heterostructure laser and channeled-substrate laser diodes (18).

Conclusion

In summary, we have studied chemical etching characteristics of (001)InP in the solutions of various systems: (*i*) HCl, (*ii*) HCl:HNO_3, (*iii*) HBr, (*iv*) H_2SO_4:H_2O_2:H_2O, and (*v*) Br_2:CH_3OH systems. The etch figures developed on (001)InP have indicated that it has untruncated tetragonal pyramid structure, in contrast to that on (001)GaAs or (001)InSb [truncated (flat-bottomed) tetragonal pyramid structure]. The etching profiles exhibiting crystal habits, *e.g.*, V-shaped groove, reverse mesa-shaped ones, and nearly vertical walls, have been found to be formed by stripes parallel to the [110] and [1̄10] directions being etched on the (001) planes. The indexes of the etch-revealed planes have been identified by making a comparison with the calculated angle between the (001) surface and etch-side plane. The etching profiles applicable to the device-structure design and fabrication have also been discussed.

Acknowledgment

The authors wish to thank Drs. M. Watanabe, T. Suzuki, M. Fujimoto, and G. Iwane for their en-

couragement throughout this work. They also thank Mr. Y. Suzuki for useful advice.

Manuscript submitted Oct. 6, 1980; revised manuscript received Dec. 22, 1980.

Any discussion of this paper will appear in a Discussion Section to be published in the December 1981 JOURNAL. All discussions for the December 1981 Discussion Section should be submitted by Aug. 1, 1981.

Publication costs of this article were assisted by Nippon Telegraph and Telephone Public Corporation.

REFERENCES

1. W. Kern, *RCA Rev.*, **39**, 227 (1978), and references therein.
2. Y. Tarui, Y. Komiya, and Y. Harada, *This Journal*, **118**, 118 (1971).
3. H. C. Gatos and M. C. Lavine, *ibid.*, **107**, 427 (1960).
4. B. Tuck and A. J. Baker, *J. Mater. Sci.*, **8**, 1559 (1973).
5. A. Huber and N. T. Linh, *J. Cryst. Growth*, **29**, 80 (1975).
6. D. Lubzens, *Electron. Lett.*, **13**, 171 (1977).
7. T. Kambayashi, C. Kitahara, and K. Iga, *Jpn. J. Appl. Phys.*, **19**, 79 (1980).
8. G. H. Olsen, M. S. Abrahams, and T. J. Zamerowski, *This Journal*, **121**, 1650 (1974).
9. H. C. Gatos and M. C. Lavine, *ibid.*, **107**, 433 (1960).
10. S. Iida and K. Ito, *ibid.*, **118**, 768 (1971).
11. M. Otsubo, T. Oda, H. Kumabe, and H. Miki, *ibid.*, **123**, 676 (1976).
12. L. Comerford and P. Zory, *Appl. Phys. Lett.*, **25**, 208 (1974).
13. W. T. Tsang and S. Wang, *ibid.*, **28**, 44 (1976).
14. J. J. Gannon and C. J. Nuese, *This Journal*, **121**, 1215 (1974).
15. J. L. Merz, R. A. Logan, and A. M. Sergent, *IEEE J. Quantum Electron.*, **qe-15**, 72 (1979).
16. P. D. Wright, R. J. Nelson, and T. Cella, *Appl. Phys. Lett.*, **36**, 518 (1980), and references therein.
17. B. I. Miller and K. Iga, *ibid.*, **37**, 339 (1980).
18. H. C. Casey, Jr., and M. B. Panish, "Heterostructure Lasers," Part B, pp. 156-276, Academic Press, New York (1978).

Auger Depth Profile Studies of Diffusion at Iron Phthalocyanine/Copper Phthalocyanine Interfaces

Robert E. Davis[*] **and Larry R. Faulkner**[**]

Department of Chemistry and Materials Research Laboratory, University of Illinois, Urbana, Illinois 61801

ABSTRACT

Elemental depth profiles of thin molecular films have been obtained using Auger electron spectroscopy in conjunction with ion etching by reducing the average electron current density and using a conducting substrate. The minimum observed interface width of CuPc (800Å thick)/FePc (800Å thick) in unannealed samples was approximately 300-400Å. Evidence is presented that this broad interface is due to the microcrystalline morphology of these physically vapor-deposited molecular solids. Annealing under various conditions has provided insight into the diffusion and consequent degradation of these assemblies, apparently through a grain boundary mechanism.

Thin molecular films have been utilized recently as means for organizing a variety of chemical systems, including modified electrodes and photoelectrochemical devices (1-8). Although surface analysis techniques such as x-ray photoelectron spectroscopy (XPS or ESCA) have been used effectively to characterize the surfaces of such systems (5, 7, 9, 10), there is a crippling lack of knowledge about the validity of methods for characterizing them as a function of depth. Auger electron spectroscopy, with ion-beam etching, and secondary ion mass spectrometry have been widely employed for that purpose in dealing with multilayer assemblies of thin films of conventional materials, such as metals and semiconductors (11, 12). However, with molecular materials there is added concern over artifacts resulting from molecular degradation (13) and diffusional mixing (14) under the beams of charged particles.

In this paper, we communicate the successful Auger depth profiling of phthalocyanine (Pc) thin films, which are interesting for their electrocatalytic (15-18) and photovoltaic (6, 19, 20) properties. The results suggest that accurate profiles, without artifacts from beam damage, can be obtained. Data from annealed samples provide information about diffusional degradation of the film assemblies.

Experimental

The samples were prepared by physical vapor deposition in a vacuum of less than 10^{-6} Torr using a commercially available bell jar (Varian Model 3117). First, silver (3000Å) was deposited onto 1×1 in. microscope cover glasses (Corning No. 2) held at room temperature. This layer was intended to provide for thermal and electrical conduction away from the semiconducting thin layers ($\sim$800Å each) of two different metal phthalocyanines, which were vapor deposited next at rates from 0.5 to 1 Å-sec^{-1} from quartz or alumina crucibles heated to $\sim$400°. Changing of the deposition source necessitated exposure of the samples to the atmosphere between each step. Film thickness and deposition rate were monitored by a quartz crystal balance (Sloan DTM-200) and verified by interferometry (Varian Å-scope).

Analysis was done at a typical background pressure of 2×10^{-9} Torr with a scanning Auger microprobe (Physical Electronics Model 545). Excitation was by a coaxial 3 keV electron beam, typically of 2.0 μA. The electron beam of 20-40 μm diam) was rastered over an area approximately 167×167 μm to reduce the average current density. Ion etching was obtained with 60 μA/cm^2 of 1 keV argon from a single, 20.7° off-normal ion gun at a rate of approximately 20 Å/min. We will use the term sputtering with caution in the current context of molecular solids. Argon ion etching of polymers has been shown to be a very complex process, involving

---

[*] Electrochemical Society Student Member.
[**] Electrochemical Society Active Member.

Key words: analysis, organic, films, sputtering.